A major purpose of the Technical Information Center is to provide the broadest dissemination possible of information contained in DOE's Research and Development Reports to business, industry, the academic community, and federal, state and local governments.

Although a small portion of this report is not reproducible, it is being made available to expedite the availability of information on the research discussed herein.

1

LA-UR 90-1596

CONF 9003164--1

JUN 1 1 1990

LA-UR--90-1596

DE90 011961

TITLE: RF PROPERTIES OF HIGH TEMPERATURE SUPERCONDUCTORS: CAVITY METHODS

AUTHOR(S):

A. M. PORTIS
UNIVERSITY OF CALIFORNIA AT BERKELEY

D. W. COOKE AND E. R. GRAY
LOS ALAMOS NATIONAL LABORATORY

SUBMITTED TO: SYMPOSIUM ON HIGH TEMPERATURE SUPERCONDUCTORS IN HIGH FREQUENCY FIELDS
WILLIAMSBURG, VA
MARCH 28-30, 1990

JOURNAL OF SUPERCONDUCTIVITY

Presented at the *Symposium on High Temperature Superconductors in High Frequency Fields,* Williamsburg, VA, 28-30 March 1990. To be published in the October 1990 issue of the *Journal of Superconductivity,* Plenum Publishing Corp.

RF Properties of High Temperature Superconductors: Cavity Methods

A. M. Portis,[1] D. W. Cooke[2] and E. R. Gray[2]

Received 28 March 1990

A description of cavities used in the study of the microwave properties of the high-temperature superconductors is followed by a lumped-circuit analysis of the coupling of transmission lines and resonators. The frequency dependence of the reflected and transmitted microwave power and the character of transient cavity response are analyzed. Techniques are discussed for the introduction of samples of the high-temperature superconductors into microwave cavities. Following a discussion of sample surface impedance and sample geometry factor, the connection between surface resistance and cavity Q is examined as well as the connection between cavity frequency shift and surface reactance. Measurement techniques that utilize reflected or transmitted power or transient response are described.

KEY WORDS: *high-temperature superconductivity*
microwave cavities
sample surface impedance

[1]University of California at Berkeley, Berkeley, CA 94720

[2]Los Alamos National Laboratory, Los Alamos, NM 87545

1. CAVITY RESONATORS

1.1. Introduction

Microwave cavity resonators are enclosed structures that support a resonant electromagnetic mode at microwave frequencies . The simplest cavities are resonant sections of transmission lines. The earliest use of microwave cavities to study the electrodynamics of superconductors was the work of Pippard [1].

1.2. Circular Cylindrical Resonators

Modes of a cylindrical resonator of length d are designated as TE_{mnp} or TM_{mnp} with

$$(\omega/c)^2 = k_{mn}^2 + (p\pi/d)^2 \tag{1}$$

where $k_{mn}= 2\pi/\lambda_{mn}$ is the appropriate cutoff wavevector and p is the number of half wavelengths along the axis of the cavity. The modes of a circular cylindrical cavity are characterized by the radial and azimuthal dependence of the longitudinal component of field. The degeneracy of the circular TM_{1np} and TE_{0np} modes must be lifted by modification of an end wall .

Bohn *et al.* [2,3] have constructed six circular Cu and Nb cavities resonant in TE_{011} and TE_{012} modes at frequencies from 1.5 to 40 GHz. Centered in the top plate is a hole that lifts the degeneracy of the TE_{01p} and TM_{11p} modes. The sample replaces the end wall of the cavity as is discussed in Sec. 3.1. An advantage of the TE_{01p} modes is that the electric field is entirely azimuthal with no radial component. So long as circular symmetry is preserved no currents cross joints normal to the cylinder axis.

Rubin *et al.* [4] have built a superconducting niobium 6 GHz circular TE_{011} cavity with removable endplates. A groove is placed in one of the endplates to lift the degeneracy with the TM_{111} mode. A pair of coupling loops are located in the upper endplate. The input loop is variable while the output loop, which monitors the transmitted power and the transient decay, is fixed. The opposite end plate contains a niobium tube that is beyond cutoff. The sample is mounted on a small-diameter sapphire rod on the axis of the tube. The extension of the sample into the cavity is varied externally.

Sridhar and Kennedy [5] have used a circular TE_{011} cavity constructed of oxygen-free high-conductivity (OFHC) copper. The cavity is held at 4.2 K with the sample, similarly mounted on a sapphire rod, at elevated temperature. Microwave radiation is coupled into and out of the resonator through two coaxial lines, each terminated by a loop within circular cutoff tubes. Coupling to the resonator is varied by moving the loops in and out of their cutoff tubes.

Müller *et al.* [6] have developed an OFHC copper cavity with a circular TE_{021} mode at 86 GHz and a circular TE_{013} mode at 87 GHz. Carini *et al.* [7,8] have constructed millimeter-wave copper transmission cavities resonant in a circular TE_{011} mode at 102 and 148 GHz.

1.3. Rectangular Resonators

The modes of a resonator of rectangular cross-section are designated as rectangular TE_{mnp} or TM_{mnp} where m and n indicate the number of nodes in the longitudinal field along the rectangular axes and p indicates the number of half wavelengths contained by the cavity. TE and TM modes with the same indices are degenerate except for m or n equal to 0 for which there can be no TE mode.

Microwave spectrometers for the observation of electron spin resonance have commonly used cavities resonant in TE_{10p} modes [9-11]. Fuller *et al.* [12] and Rachford *et al.* [13] have placed samples on the walls of their rectangular TE_{103} copper cavity resonant at 9.2 GHz. Microwave power is coupled into the cavity by means of a Gordon coupler [14], which may be adjusted externally.

1.4. Coaxial TEM Resonators

Measurements on bulk superconductors at frequencies below 1.7 GHz may usefully be made with a half-wave coaxial resonator. The outer conductor can be copper with cavity losses dominated by the sample, a superconducting axial rod. The entire apparatus may be filled with either liquid nitrogen or liquid helium. An important advantage of this arrangement is that the considerable heat generated by the sample in high-power critical rf field measurements is readily transferred to the cryogen.

Argonne investigators [2,15] have measured thin cylindrical rods of $YBa_2Cu_3O_{7-\delta}$ contained by a quartz tube on the axis of a half-wave resonant coaxial line. The line is shielded by a copper outer conductor. The outer cylinder extends beyond the ends of the inner conductor and in these regions acts as a circular TM_{01} transmission line beyond cutoff. Two cavities have been constructed, one for operation in the frequency range 150-600 MHz and the second in the range 600-1500 MHz.

The advantages of the coaxial cavity are (i) its transverse dimensions may be quite small, (ii) high surface fields can be achieved at the inner conductor with moderate power input leading to high sensitivity and (iii) it is not necessary for the shield to be superconducting.

2. COUPLING OF TRANSMISSION LINES AND RESONATORS

We begin with a summary of the results of transmission line theory, where waveguides and coaxial cables are represented by distributed-element transmission lines and the microwave resonator by a lumped-element circuit. The coupling of the transmission lines to the resonator is represented by ideal transformers.

2.1. Transmission Lines

The Telegraphist's Equations [16] describe the relation between the voltage V across a transmission line and the current I that flows through the line and leads to the expression for the characteristic impedance of the line

$$Z_0 = V/I = \omega L/\beta = \sqrt{L/C} \quad (2)$$

where L is the series inductance per unit length, C is the shunt capacitance per unit length and $\beta = \omega\sqrt{LC}$ is the wavevector of the line.

Terminating the line with an impedance Z_L leads to a terminal voltage V_L and terminal current I_L satisfying

$$V_L = I_L Z_L = [(1+\rho)/(1-\rho)] I_L Z_0 \tag{3}$$

where ρ is the complex reflection coefficient. Assuming an incident wave of amplitude $^1/_2 V_0$, the reflection coefficient is

$$\rho = 2\frac{V_L}{V_0} - 1 = \frac{Z_L - Z_0}{Z_L + Z_0} \tag{4}$$

The voltage at the load is that generated by a voltage source V_0 with internal impedance Z_0 working directly into a lumped-element load Z_L.

2.2. Equivalent Circuit

The equivalent circuit of a resonator coupled to input and output transmission lines is shown in Fig. 1 (a). The magnetic energy stored in the resonator is associated with the inductor L. The electrical energy is associated with the capacitor C, and dissipation is through the resistor R. An equivalent circuit is taken with the three elements in parallel. Coupling to the input transmission line of characteristic impedance Z_0 is through an ideal transformer with turns-ratio m:1. The resonator is loaded by an output line of impedance Z_0' through an ideal transformer of turns-ratio m':1. The microwave source is matched to the input line and represented by a voltage generator V_0. The detector is matched to the output line.

The reciprocal impedance of the unloaded resonator is

$$1/Z = 1/R + i\ (1/\omega L - \omega C) \tag{5}$$

The complex resonant frequency is at the zero of Z

$$\omega = [\omega_0^2 - 1/(2\tau)^2]^{1/2} - i/2\tau \tag{6}$$

with $\omega_0 = 1/\sqrt{LC}$ and energy relaxation time $\tau = RC$. The unloaded quality factor of the resonator is defined as

$$Q_u = \omega_0\tau = R/\omega_0 L \tag{7}$$

2.3. Resonator Response

The expected response of a resonator is best studied by transforming the driving voltage and loads into shunt with the resonator as shown in Fig. 1 (b). In parallel with R are the load resistances m^2Z_0 and m'^2Z_0'. We characterize these loads by external quality factors

$$Q_e = m^2Z_0/\omega_0L = Q_u/\beta \qquad Q_e' = m'^2Z_0'/\omega_0L = Q_u/\beta' \tag{8}$$

The total cavity loss is represented by the loaded quality factor Q_ℓ with

$$1/Q_\ell = 1/Q_u + 1/Q_e + 1/Q_e' \tag{9}$$

The voltage V across the resonator terminals

$$V = \frac{1/Q_e}{1/Q_\ell + i(\omega_0/\omega - \omega/\omega_0)} V_0 \tag{10}$$

is a measure of the response of the resonator.

2.4. Reflection

The voltage reflection coefficient ρ is obtained by treating the resonator as a load. From Eq. (4), the voltage at a load is $V_L = {}^1/_2\,(1 + \rho)\, V_0$ which gives

$$\rho = \frac{(2/Q_e - 1/Q_\ell) - i(\omega_0/\omega - \omega/\omega_0)}{1/Q_\ell + i(\omega_0/\omega - \omega/\omega_0)} \tag{11}$$

Both Q_e and Q_ℓ can be determined from the power reflection coefficient

$$R = |\rho|^2 = \frac{(2/Q_e - 1/Q_\ell)^2 + (\omega_0/\omega - \omega/\omega_0)^2}{(1/Q_\ell)^2 + (\omega_0/\omega - \omega/\omega_0)^2} \tag{12}$$

2.5. Transmission

The voltage transmission coefficient τ is the fractional voltage transmitted through an inserted resonator to a matched load. The power transmission coefficient $T = |\tau|^2$ is the ratio of the power delivered through the resonator to the incident power

$$T = P'/P_0 = (|V|^2/m'^2Z_0')/(V_0^2/4Z_0) \tag{13}$$

Using Eq. (3-16) the power transmission coefficient is

$$T = -\frac{4 / Q_e Q_e'}{1/Q_\ell^2 + (\omega_0/\omega - \omega/\omega_0)^2} \quad (14)$$

The bandwidth $2\delta\omega$ of the power transmission coefficient is the full frequency interval between half-power points. The half power condition from Eq. (14) is $\omega/\omega_0 - \omega_0/\omega = \pm 1/Q_\ell$. With $\omega = \omega_0 \pm \delta\omega$ we obtain from Eq. (14) for the half-width at half-power

$$2\delta\omega = \omega_0/Q_\ell \quad (15)$$

Measuring the bandwidth $2\delta\omega$ of the power transmitted through the resonator gives the loaded quality factor Q_ℓ. Comparing the transmitted power from Eq. (3-23) gives

$$\Delta T/T = \Delta Q_\ell{}^2/Q_\ell{}^2 \approx -2Q_\ell \, \Delta\,(1/Q_\ell) \quad (16)$$

2.6. Relaxation

Measurement of the power relaxation time provides a further method of determining Q_ℓ. The power relaxation time is determined by applying power to the resonator for a sufficiently long time that the response is steady and then terminating the drive power. The voltage across the resonator decays at a frequency $\omega = \omega_0\sqrt{1 - 1/4Q_\ell^2}$ with a power relaxation time given by

$$\tau = Q_\ell/\omega_0 \quad (17)$$

Comparison with Eq. (15) gives for the full-width at half-power $2\delta\omega = 1/\tau$. Sridhar and Kennedy [5] have described the electronics for measuring the resonator decay time τ.

3. SAMPLE CONFIGURATIONS

3.1. Replacement

In the replacement configuration, the end wall, usually of a circular TE_{011} cavity, is replaced by a thick superconducting film or a film deposited on a metallic conductor. In this geometry no currents flow across the junction between the end wall and the body of the cylindrical cavity and there are no additional losses. Delayen *et al.* [15]

have replaced the copper center rod of their coaxial cavity by ceramic superconducting rods.

Bohn *et al.* [2,3] have used samples ranging from 1.25 to 15 cm in diameter to form the bottom end wall of an appropriate size cavity. Cooke *et al.* [17,18] obtain the temperature dependence of the surface resistance R_s of the end wall of a copper cavity by cooling to T = 15 K with a closed-cycle refrigerator and slowly warming to room temperature while measuring Q values. A computer-controlled network analyzer automatically determines the resonance peak and half-power points from which the cavity quality factor is calculated.

Radcliffe *et al.* [19] have used a clamped ceramic superconducting disk as a replacement for the end wall of a circular brass transmission cavity. A number of the approximately sixty detectable modes in the frequency range 7 to 20 GHz were selected. Under computer control, the power transmission coefficient, bandwidth and frequency were measured between 4.2 K and room temperature.

Carini *et al.* [7,8] have measured surface impedance in TE_{011} transmission cavities at the millimeter-wave frequencies 102 and 148 GHz. The sample was mounted as the end wall of the cavity and the power transmitted through the cavity was measured as a function of microwave frequency, giving the central frequency ω_0 and the bandwidth $2\delta\omega$.

3.2. Cavity Perturbation

Specimens may be measured in a cavity by the perturbation method with the electromagnetic field penetrating either one or both surfaces of the sample depending on sample placement.

Rubin *et al.* [4] have measured the temperature dependence of the surface resistance of ceramic pellets in a superconducting niobium 6 GHz circular TE_{011} resonant cavity. As described in Sec. 1.2, samples are mounted on a sapphire rod enclosed by a niobium cutoff tube. The sapphire rod makes contact with the helium bath through a thermal resistor. Magnetic fields in the TE_{011} mode are radial at the end wall and vanish on axis. For this reason the contribution of a small-diameter sample to the increase in cavity losses is substantially reduced. By measuring the rise in the temperature of a thermal resistor half-way up the sapphire rod, Rubin *et al.* [4] detect resistances 100 times smaller than can be measured from the reduction in cavity Q. Rubin *et al.* [20] have examined the microwave properties of a number of small single crystals that were attached to the end of the sapphire rod and the cavity Q was measured as a function of crystal temperature.

Awasthi *et al.* [21] and Carini *et al.* [8] have measured the temperature dependence at millimeter-wave frequencies of the surface impedance of ceramic superconductors. The surface resistance is determined from the change in $1/Q_\ell$, as discussed in Sec. 4.2. The penetration depth is computed from the surface reactance, which produces a shift in cavity frequency that is discussed in Sec. 4.3.

3.4. All High-T_c Cavity

Zahopoulos *et al.* [22] have constructed an all-high-T_c circular TE_{011} cavity, dielectrically loaded with sapphire in order to reduce the dimensions for resonance at 8.0 GHz. Dielectrically loaded resonators of reduced volume have similarly been used for magnetic resonance [23,24]. The loaded quality factor Q_ℓ was measured by the decay method [5] between room temperature and 4.2 K.

Minehara *et al.* [25] have constructed from $YBa_2Cu_3O_{7-\delta}$ a circular TM_{010} microwave transmission cavity resonant at 7 GHz. The loaded Q was determined from the bandwidth of the transmitted power. The unloaded Q as a function of temperature was determined from Q_ℓ and the transmission coefficient by Eq. (14).

Radcliffe *et al.* [26] have assembled a cylindrical transmission resonator from three clamped pieces of sintered $YBa_2Cu_3O_7$ and have measured the temperature dependence of the surface resistance from 4 to 300 K for five modes in the frequency interval 10 to 18 GHz.

Gantmakher *et al.* [27,28] have also constructed a circular TE_{011} cavity resonant at 17.6 GHz entirely from $YBa_2CU_3O_{7-\delta}$. The loaded Q as a function of temperature was determined from the power transmission coefficient calibrated at one temperature from the bandwidth of the transmitted power.

4. ANALYSIS

4.1. Surface Impedance

The surface impedance of a conductor is the ratio of the electric to the magnetic field at the surface

$$Z_S = R_S - i X_S = E_S/H_S \tag{18}$$

The penetration depth λ and the classical skin depth δ may be determined from the surface impedance of a superconductor thick compared with the penetration depth

$$Z_S = -i\omega\lambda\mu/[1 - 2i(\lambda/\delta)^2]^{1/2} \tag{19}$$

This expression may require correction for microwave penetration of the substrate.

4.2. Geometry Factor.

The energy dissipated at the cavity walls is

$$P = \frac{1}{2} \int_S dS\ R_s H_s^2 \tag{20}$$

while the energy stored in the cavity may be written as the integral

$$U = \frac{1}{2} \mu_0 \int_V dV\ H^2 \tag{21}$$

The reciprocal of the unloaded cavity Q is

$$\frac{1}{Q_u} = \frac{P}{\omega_0 U} = \frac{\int_S dS H_s^2 R_s}{\omega_0 \mu_0 \int_V dV H^2} \tag{22}$$

A change in cavity losses as the result of wall replacement or the introduction of additional absorbing surface leads to

$$\Delta\frac{1}{Q_u} = \frac{\Delta P}{\omega_0 U} = \frac{\int_S dS H_s^2 \Delta R_s}{\omega_0 \mu_0 \int_V dV H^2} \tag{23}$$

The sample geometry factor is defined as

$$G = \frac{\int_{\Delta S} dS\, H_s^2}{\omega_0 \mu_0 \int_V dV\, H^2} \tag{24}$$

where ΔS is the area over which a change in R_s has been made, either by replacement of wall or axial material or by the insertion of material into the cavity. So long as the coupling is not affected by ΔR_s, Eq. (9) gives

$$\Delta(1/Q_\ell) = \Delta(1/Q_u) \tag{25}$$

and the change in surface resistance is

$$\Delta R_s = G\, \Delta(1/Q_\ell) \tag{26}$$

4.3. Frequency Shift

The connection between the change in surface reactance ΔX_s and the frequency shift $\Delta\omega_0$ is obtained from the following argument [1]. We should be able to relate $\Delta Z_s = \Delta R_s - i\,\Delta X_s$ to the change in complex frequency $\Delta(\omega_0 - i/2\tau)$. From Eqs. (17) and (26) we write

$$\Delta R_s = (G/\omega_0)\, \Delta\, (1/\tau) \tag{27}$$

The required complex relation is then

$$\Delta Z_s = \Delta R_s - i\, \Delta X_s = (2iG/\omega_0)\, \Delta(\omega_0 - i/2\tau) \tag{28}$$

which gives for the change in surface reactance

$$\Delta X_s = -2G\, \Delta\omega_0/\omega_0 \tag{29}$$

Slater [29,30] has obtained this result from an energy argument.

5. MEASUREMENT

5.1. Reflection

Rachford *et al.* [13] have determined the Q_u of circular TE_{011} and rectangular TE_{103} cavities from the frequency dependence of the reflected power by Eq. (21) with $1/Q_e' = 0$ for a reflection cavity. During an experimental run the cavity and sample temperature were allowed to rise slowly while the unloaded Q and frequency shift were computed and recorded at regular intervals.

5.2. Transmission

Cooke *et al.* [6,17] obtain the total surface resistance R_S rather than ΔR_S as in Eq. (26) from the fact that a known fraction f of the losses in their cavity occur at an end wall. Their argument is that if the end wall were lossless, the unloaded quality factor of the copper cavity Q_C would be increased by a factor 1/(1-f) which gives

$$R_S = G\Delta\frac{1}{Q_\ell} + \frac{fG}{Q_C} \qquad (30)$$

The sample geometry factor G, discussed in Sec. 4.2, is determined from Eq. (30) when a material such as stainless steel with known R_S is used as the end wall. Bohn *et al.* [3] have similarly determined R_S from the unloaded quality factor of a circular cavity operating in a TE_{011} or TE_{012} mode with the sample forming the bottom surface.

Klein *et al.* [31, 32] have determined the surface resistance and reactance of several *c*-axis oriented epitaxial thin films of $YBa_2Cu_3O_7$ at 87 GHz with a circular TE_{013} cavity through the use of Eqs. (26) and (29). Partial penetration of microwave radiation into the substrate leads to an enhancement of Z_S and must be corrected for the determination of λ and δ through Eq. (19).

Carini *et al.* [7,8] have measured the surface impedance at millimeter-wave frequencies from the power transmitted through the cavity as a function of frequency, giving the central frequency ω_0 and the bandwidth $2\delta\omega$. The procedure was repeated with a polished OFHC copper end wall. The difference between the surface resistances of the sample and copper end wall is given by Eq. (26). The difference in surface reactance is related to the shift in cavity frequency by Eq. (29).

Minehara *et al.* [25] have determined the unloaded Q of an all $YBa_2Cu_3O_{7-\delta}$ cavity from the power transmission coefficient and the bandwidth of the transmitted power. The surface resistance was obtained from Eq. (26) with $R_S = G/Q_u$, where G is the sample geometrical factor computed from Eq. (24) for a cavity in which the sample covers the entire surface.

Delayen *et al.* [15] have used coaxial cavities from 150 to 1500 MHz [3] with surface rf magnetic fields up to 640 Oe at 190 MHz at an input power of 2.2 kW with the resonant line immersed in liquid nitrogen. The surface rf magnetic field at the sample is determined from the voltage at a calbrated pickup probe located midway between the end-plates of the cavity.

5.3. Relaxation

The surface resistance as a function of temperature, frequency and power may be determined from a measurement of the decay time τ of pulsed cavity excitation. Sridhar and Kennedy [5] have fed pulsed microwave power into one port of a circular TE_{011} cavity and observed the transmitted signal, following detection, on a fast oscilloscope. The loaded quality factor of the resonator was determined from Eq. (17). The resonant frequency $\omega_0/2\pi$ was directly obtained from the synthesizer output. The surface resistance and reactance were determined by the sample perturbation relations, Eqs. (26) and (29).

Rubin *et al.* [4] take the power transmission coefficient T as a measure of the cavity unloaded Q. The rise in temperature of a niobium pellet at room temperature, where the microwave surface resistance of niobium is accurately known, gives the magnetic field strength at the pellet surface. A sintered ceramic pellet then replaces the niobium standard and the decay time is measured as a function of pellet temperature. Coupling to the cavity is adjusted to fix the rf field at the sample.

Kato *et al.* [33] determine Q_ℓ from τ on reflection from a circular TM_{011} cavity resonant at 2.86 GHz. A measurement of the the power reflection coefficient R through Eq. (12) leads to the unloaded cavity Q and $\Delta(1/Q_u)$ when the cavity is perturbed.

Delayen and Bohn [34] determined the differential decay rate $\Delta(1/\tau)$ associated with sample losses. From the known surface resistance R_s of Pb at room temperature, the sample geometry factor $G\ \Delta(1/\tau) = \omega_0\ \Delta R_s$ was determined as given by Eq. (27). The geometry factor is independent of the material properties of the central conductor, but does depend on its diameter as may be seen from Eq. (24). Replacing the sample by a copper rod yields a shorter decay time. This procedure gives the difference between R_s of the superconductor and R_s of copper [35]. The surface resistance of the superconductor may be obtained by analogy with Eq. (30)

$$R_s = G[\omega_0\ \Delta(1/\tau) + f/Q_c] \tag{31}$$

where Q_c is the unloaded Q of the cavity with copper as the center conductor and $f \approx 1$ is the fraction of unloaded loss that arises from the center conductor.

At high rf levels with the central conductor a superconducting ceramic, the pulse decay is nonexponential with a long tail. This behavior indicates that the surface resistance R_s of the ceramic increases with the strength of the rf magnetic field. Under these conditions the initial decay rate is taken as a measure of the surface resistance at peak power. The decay time may be determined as a function of rf magnetic field from the local logarithmic derivative.

ACKNOWLEDGEMENTS

The work at Berkeley was supported by the Director, Office of Energy Research, Office of Basic Energy Sciences, Materials Sciences Division, of the U.S. Department of Energy under Contract No. DE-AC03-76SF00098. Work at Los Alamos was supported by the Superconductivity Pilot Center of the U.S.Department of Energy. The Berkeley-Los Alamos collaboration was supported by the Office of the President of the University of California.

REFERENCES

1. A. B. Pippard, *Proc. Roy. Soc. (London)* **A216**, 547 (1953).
2. C. L. Bohn, J. R. Delayen and M. T. Lanagan, *Proceedings of the Workshop on High-T_c Superconductivity*, Huntsville, AL, 23-25 May 1989. GACIC Publication PR-89-02, IIT Research Institute, Chicago.
3. C. L. Bohn, J. R. Delayen, U. Balachandran and M. T. Lanagan, *Appl. Phys. Lett.* **55**, 304 (1989).
4. D. L. Rubin, J. Gruschus, J. Kirchgessner, D. Moffat, H. Padamsee, J. Sears, Q. S. Shu, S. Thoʻen, E. Wilkins, R. Buhrman, S. Russek and T. W. Noh, *Proceedings of the Third Workshop on rf Superconductivity,* Argonne, IL, September 1987, edited by K. W. Shepard, Argonne National Laboratory Publication ANL-PHY-88-1. Pages 211-227.
5. S. Sridhar and W. L. Kennedy, *Rev. Sci. Instrum.* **59**, 531 (1988).
6. G. Müller, D. J. Brauer, R. Eujen, M. Hein, N. Klein, H. Piel, L. Ponto, U. Klein and M. Peiniger, *IEEE Trans. Magn.* **25**, 2402 (1989).
7. J. P. Carini, A. N. Awasthi, W. Beyermann, G. Grüner, T. Hylton, K. Char, M. R. Beasley and A. Kapitulnik, *Phys. Rev. B* **37**, 9726 (1988).
8. J. Carini, L. Drabeck and G. Grüner, *Mod. Phys. Lett.* **3**, 5 (1989).
9. D. J. E. Ingram, *Spectroscopy at Radio and Microwave Frequencies, Second Edition,* Butterworths, London, 1967.
10. C. P. Poole, Jr., *Electron Spin Rosonance, A Comprehensive Treatise on Experimental Techniques,* Interscience Publishers, New York, 1967.
11. R. S. Alger, *Electron Paramagnetic Resonance: Techniques and Applications,* Interscience Publishers, New York, 1968.
12. W. W. Fuller, F. J. Rachford, W. L. Lechter, P. R. Broussard, L. H. Allen and J. H. Classen, *IEEE Trans. Magn.* **25**, 2394 (1989).
13. F. J. Rachford, W. W. Fuller and M. S. Osofsky, *J. Supercond.* **1**, 165 (1988).

14. J. P. Gordon, *Rev. Sci. Instrum.* **32**, 658 (1961).

15. J. R. Delayen, K. C. Goretta, R. B. Poeppel and K. W. Shepard, *Appl. Phys. Lett.* **52**, 930 (1988).

16. S. Ramo, J. R. Whinnery and T. Van Duzer, *Fields and Waves in Communication Electronics, Second Edition* (John Wiley & Sons, New York, 1984). Sections 8.11, 10.10 and 11.14.

17. D. W. Cooke, E. R. Gray, R. J. Houlton, B. Rusnak, E. A. Meyer, J. G. Beery, D. R. Brown, F. H. Garzon. I. D. Raistrick, A. D. Rollett and R. Bolmaro, *Appl. Phys. Lett.* **55**, 914 (1989).

18. D. W. Cooke, E. R. Gray, R. J. Houlton, H. H. S. Javadi, M. A. Maez, B. L. Bennett, B. Rusnak, E. A. Meyer, P. N. Arendt, J. G. Beery, D. R. Brown, F. H. Garzon, I. D. Raistrick, A. D. Rollett, B. Bolmaro, N. E. Elliott, N. Klein, G. Müller, S. Orbach, H. Piel, J. Y. Josefowicz, D. B. Rensch, L. Drabeck and G. Grüner, *Physics C* **162-164**, 1537 (1989).

19. W. J. Radcliffe, J. C. Gallop, C. D. Langham, M. Gee and M. Stewart, *Physica C* **153-155**, 635 (1988).

20. D. L. Rubin, K. Green, J. Gruschus, J. Kirchgessner, D. Moffat, H. Padamsee, J. Sears, Q. S. Shu, L. F. Schneemeyer and J. V. Waszczak, *Phys. Rev. B* **38**, 6538 (1988).

21. A. M. Aswasthi, J. P. Carini, B. Alavi and G. Grüner, *Solid State Commun.* **67**, 373 (1988).

22. C. Zahopoulos, W. L. Kennedy and S. Sridhar, *Appl. Phys. Lett.* **52**, 2168 (1988).

23. W. W. Walsh, Jr. and L. W. Rupp, Jr., *Rev. Sci. Instr.* **57**, 2778 (1986).

24. R. W. Dykstra and G. D. Markham, *J. Mag. Res.* **69**, 350 (1986).

25. E. Minehara, R. Nagai and M. Takeuchi, *Jpn. J. Appl. Phys.* **28**, L100 (1989).

26. W. J. Radcliffe, J. C. Gallop, C. D. Langham, M. Gee and M. Stewart, *IEEE Trans. Magn.* **25**, 990 (1989).

27. V. F. Gantmakher, V. I. Kulakov, G. I. Leviev, R. K. Nikolaev, A. V. Polisskii, N. S. Sidorov, *Soc. Phys. JETP* **68**, 833 (1989).

28. V. F. Gantmakher, V. I. Kulakov, G. I. Leviev, R. K. Nikolaev, A. V. Polisskii, N. S. Sidorov, *Physica C* **162-164**, 1539 (1989).

29. J. C. Slater, *Microwave Electronics* (D. Van Nostrand Co., Inc., New York, 1950). See also J. C. Slater, *Revs. Mod. Phys.* **18**, 441 (1946).

30. J. C. Slater, *Microwave Transmission* (McGraw-Hill Book Company, Inc., New York, 1942; reprinted by Dover Publications, New York, 1959).

31. N. Klein, G. Müller, H. Piel, B. Roas, L. Schultz, U. Klein and M. Peiniger, *Appl. Phys. Lett.* **54**, 757 (1989).

32. N. Klein, G. Müller, S. Orbach, H. Piel, H. Chaloupka, B. Roas, L. Schultz, U. Klein and M. Peiniger, *Physica C* **162-164**, 1549 (1989).

33. K. Kato, K. Takahashi, H. Mitera and K. Minami, *Jpn. J. Appl. Phys.* **27**, 1641 (1988).

34. J. R. Delayen and C. L. Bohn, *Phys. Rev.* **40**, 5151 (1989).

35. J. R. Delayen, K. W. Shepard, K. C. Goretta and R. B. Poeppel, *Proceedings of the Third Workshop on rf Superconductivity*, Argonne, IL, September 1987, edited by K. W. Shepard, Argonne National Laboratory Publication ANL-PHY-88-1.

Figure Legends

Fig. 1. (a) Equivalent circuit of a two-port resonator coupled to input and output transmission lines. The magnetic energy stored in the resonator is associated with the inductor L. The electrical energy is associated with the capacitor C, and dissipation is through the resistor R. The resonator is driven from an input line of impedance Z_0 through an ideal transformer of turns ratio 1:m and loaded by an output line of impedance Z_0' through an ideal transformer of turns ratio m':1. The microwave source

is matched to the input line and represented by a voltage generator V_0. The detector is matched to the output line.

(b) Transformation of the driving voltage and loads into shunt with the resonator. In parallel with R are the load resistances m^2Z_0 and m'^2Z_0'.

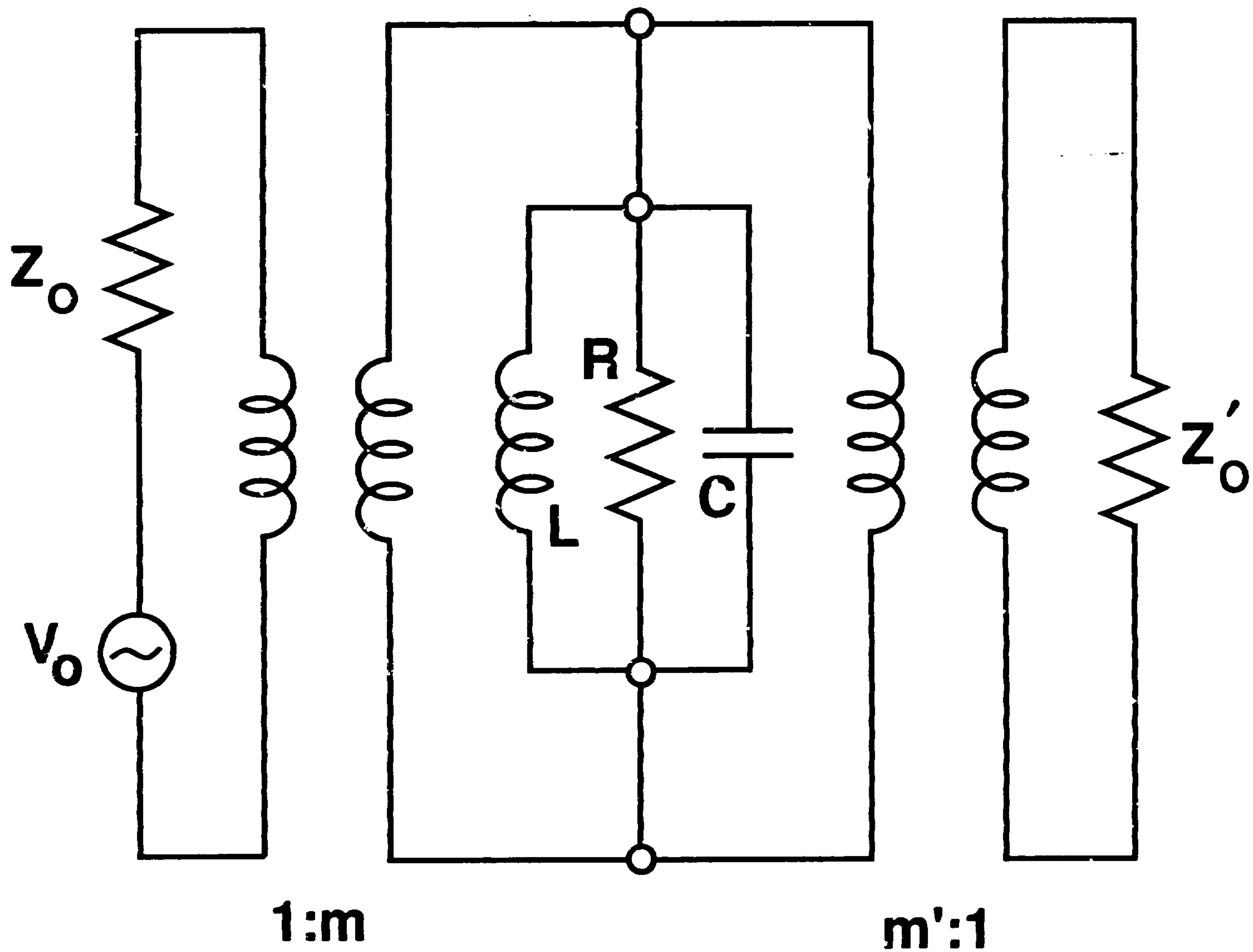

Z_o
V_o
R
L
C
Z_o'
1:m
m':1

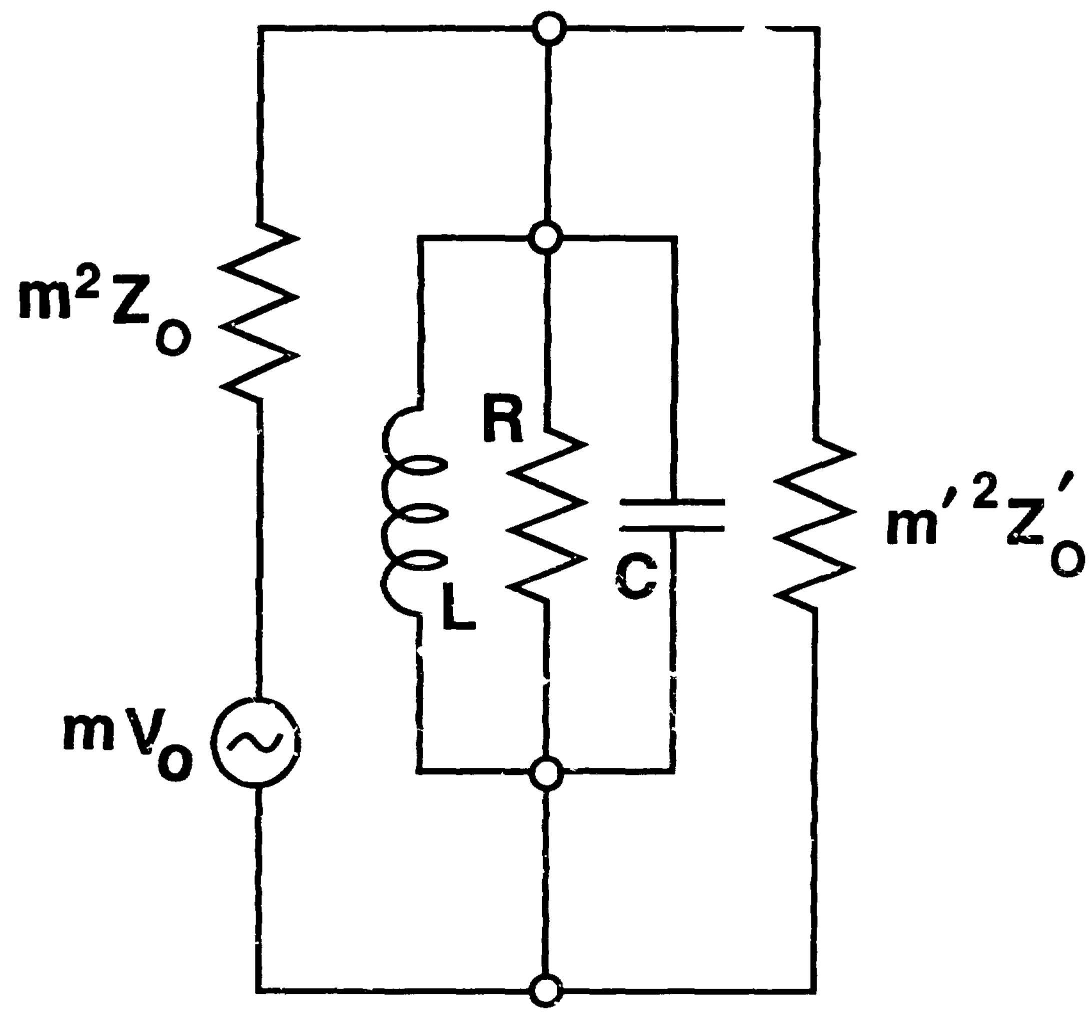

m²Z₀
R
L
C
m′²Z′₀
mV₀